**Cell Death and Differentiation (2017) 24,** 649–659
 1350-9047/17

www.nature.com/cdd

# KCTD2, an adaptor of Cullin3 E3 ubiquitin ligase, suppresses gliomagenesis by destabilizing c-Myc

**Eun-Jung Kim[1,2,6], Sung-Hak Kim[3,6], Xiong Jin[1,2], Xun Jin[4,5] and Hyunggee Kim[*,1,2]**

**Cullin3 E3 ubiquitin ligase ubiquitinates a wide range of substrates through substrate-specific adaptors Bric-a-brac, Tramtrack, and Broad complex (BTB) domain proteins. These E3 ubiquitin ligase complexes are involved in diverse cellular functions. Our recent study demonstrated that decreased Cullin3 expression induces glioma initiation and correlates with poor prognosis of patients with malignant glioma. However, the substrate recognition mechanism associated with tumorigenesis is not completely understood. Through yeast two-hybrid screening, we identified potassium channel tetramerization domain-containing 2 (KCTD2) as a BTB domain protein that binds to Cullin3. The interaction of Cullin3 and KCTD2 was verified using immunoprecipitation and immunofluorescence. Of interest, KCTD2 expression was markedly decreased in patient-derived glioma stem cells (GSCs) compared with non-stem glioma cells. Depletion of KCTD2 using a *KCTD2*-specific short-hairpin RNA in U87MG glioma cells and primary *Ink4a/Arf*-deficient murine astrocytes markedly increased self-renewal activity in addition with an increased expression of stem cell markers, and mouse *in vivo* intracranial tumor growth. As an underlying mechanism for these KCTD2-mediated phenotypic changes, we demonstrated that KCTD2 interacts with c-Myc, which is a key stem cell factor, and causes c-Myc protein degradation by ubiquitination. As a result, KCTD2 depletion acquires GSC features and affects aerobic glycolysis via expression changes in glycolysis-associated genes through c-Myc protein regulation. Of clinical significance was our finding that patients having a profile of *KCTD2* mRNA-low and c-Myc gene signature-high, but not KCTD2 mRNA-low and c-Myc mRNA-high, are strongly associated with poor prognosis. This study describes a novel regulatory mode of c-Myc protein in malignant gliomas and provides a potential framework for glioma therapy by targeting c-Myc function.**
*Cell Death and Differentiation* (2017) **24,** 649–659; doi:10.1038/cdd.2016.151; published online 6 January 2017

The polyubiquitination and subsequent degradation of cellular proteins in proteasomes have a key role in many biological processes. In fact, dysregulation of the protein degradation system contributes to many cancers.[1] The ubiquitination-dependent protein degradation system is a 3-step process. Ubiquitin is activated by an E1 ubiquitin-activating enzyme. The activated ubiquitin is transferred by an E2 ubiquitin-conjugating enzyme to the targeted protein, where it binds to lysine residues of the substrate by E3 ubiquitin ligase. E3 ubiquitin ligase complexes are classified into two families according to their domain: homologous to the E6-AP carboxyl terminus (HECT) domain ligases or really interesting new gene (RING) finger domain ligases.[2]

The Cullin protein serves as a scaffold to connect two functional modules of E3 ubiquitin ligase, the catalytic RING-finger protein and the substrate-binding molecule. Cullin-RING ubiquitin ligases are the largest E3 ligase family in eukaryotes.

Cullin3, one of the RING-finger E3 ubiquitin ligase complexes, has an essential role in embryo development, cancer progression, and many other diseases.[3] Substrate specificity of Cullin3 is determined by substrate-specific adaptors that contain the Bric-a-brac, Tramtrack, and Broad complex (BTB) domain. There are nearly 200 BTB domain proteins in humans; however, not all BTB domain proteins interact with Cullin3.[4,5]

Polyubiquitination and subsequent protein degradation have fundamental roles in many physiological and pathological processes including tumorigenesis. Malignant gliomas including glioblastoma (GBM, WHO grade IV) are the most aggressive form of brain tumors. Despite considerable progress in diagnosis, surgery, and treatment over the past several decades, the median survival time of patients with GBM is $<14$ months following diagnosis.[6] Glioma stem cells (GSCs) are a sub-population of GBMs and are capable of tumor initiation, progression, and recurrence following therapy.[7,8] Our recent study found that Cullin3 exerts a tumor-suppressor function in gliomagenesis by inhibiting the WNT and Sonic hedgehog (SHH) signaling pathways through degradation of disheveled segment polarity protein 2 (DVL2) and GLI family zinc-finger protein 2 (GLI2), respectively.[9] However, the regulation of target proteins by the Cullin3–adaptor complex and their effects on malignant gliomas are not fully understood.

[1]Department of Biotechnology, School of Life Sciences and Biotechnology, Korea University, Seoul, Republic of Korea; [2]Institute of Animal Molecular Biotechnology, Korea University, Seoul, Republic of Korea; [3]Department of Animal Science, College of Agriculture and Life Sciences, Chonnam National University, Gwangju, Republic of Korea; [4]Tianjin Medical University Cancer Institute and Hospital, Tianjin, China and [5]Institute of Translational Medicine, First Affiliated Hospital of Wenzhou Medical University, Wenzhou, Zhejiang, China

*Corresponding author: H Kim, Department of Biotechnology, School of Life Sciences and Biotechnology, Korea University, 145 Anam-Ro, Seongbuk-Gu, Seoul 02841, Republic of Korea. Tel: +82 2 3290 3059; Fax: +82 2 953 0737; E-mail: hg-kim@korea.ac.kr

[6]These authors contributed equally to this work

Received 20.8.16; revised 09.11.16; accepted 01.12.16; Edited by JP Medema; published online 06.1.2017

c-Myc is a transcription factor that has a central role in various cellular processes involving cell proliferation, glycolytic metabolism, differentiation, and apoptosis.[10] c-Myc expression and function are tightly regulated in normal cells, whereas dysregulation of c-Myc expression has been implicated in the genesis of most human cancers.[11] Moreover, overexpression of c-Myc has an important role in gliomagenesis and its progression by generating GSCs.[12] However, the precise regulatory mechanism of c-Myc expression remains largely undetermined in malignant gliomas.

In this study, we found that potassium channel tetramerization domain-containing 2 (KCTD2) is an adaptor for the Cullin3 E3 ubiquitin ligase and that it degrades c-Myc through polyubiquitination. When KCTD2 expression was depleted in glioma cells and immortalized murine astrocytes, we found that these cells acquired GSC-like properties through increases in c-Myc protein. This regulatory mechanism of c-Myc expression by Cullin3-KCTD2 may provide an alternative therapeutic strategy in targeting GSCs for malignant glioma regression.

## Results

**Identification of KCTD2 as an adaptor of Cullin3 E3 ubiquitin ligase.** Recently, our group found that suppression of Cullin3 E3 ubiquitin ligase activates GSC proliferation, self-renewal, and tumorigenicity.[9] To further understand the molecular mechanisms governing substrate recognition of Cullin3, we performed yeast two-hybrid (Y2H) screening to identify adaptor proteins that interact with Cullin3. A human fetal brain cDNA library was screened using full-length Cullin3 as bait. We identified six BTB domain-containing proteins (Figure 1a). As decreased Cullin3 promotes tumorigenesis by activating GSC properties, we hypothesized that adaptor proteins expressed at low levels in GSCs compared with non-stem glioma cells (hereafter, referred to as glioma cells) may be involved in Cullin3-driven GSC genesis. Therefore, we first compared expression levels of these adaptors in four normal astrocytes, five glioma cells, and seven GSCs using transcriptome microarray data.[13] We found that only KCTD2 mRNA levels were lower in glioma cells and GSCs compared with normal astrocytes, and significantly lower in GSCs relative to glioma cells (Figure 1b). Quantitative reverse transcription polymerase chain reaction (qRT-PCR) analysis showed that expression levels of KCTD2 mRNA were markedly lower in all 10 GSCs tested compared with 4 out of 6 glioma cells (Figure 1c). Although mass spectrometry previously suggested KCTD2 was a putative adaptor for Cullin3,[14] there was no evidence of a direct interaction. In this study, we focused on determining whether KCTD2 is a putative tumor suppressor. We first confirmed direct interaction of KCTD2 with Cullin3. One-on-one Y2H analysis was performed using selective growth medium. Yeast can colonize media lacking leucine and tryptophan through vector transformation. However, if Cullin3 interacts with KCTD2, colonies can form on media deficient in four amino acids. As further support, their binding ability was confirmed using $\beta$-galactosidase ($\beta$-gal) staining (Figure 1d).

In addition, a co-immunoprecipitation assay demonstrated an interaction between KCTD2 and Cullin3 in HEK 293 T cells (Figure 1e). Colocalization of KCTD2 and Cullin3 was examined using immunofluorescence. The results showed that both KCTD2 and Cullin3 are co-located in cytoplasm (Figure 1f). Taken together, our results show that KCTD2 is an adaptor of Cullin3 E3 ubiquitin ligase, and based on its low expression in GSCs, is a putative GSC inhibitor.

**KCTD2 interacts with c-Myc and reduces its protein level.** As our previous study demonstrated that Cullin3 suppresses SHH and WNT signaling through ubiquitination-dependent degradation of GLI2 and DVL2, respectively,[9] we tested whether KCTD2 was involved in GLI2 and DVL2 degradation. Western blot analysis found that KCTD2 knockdown using a *KCTD2*-specific short-hairpin RNA (shRNA) did not change GLI2 and DVL2 protein levels in U87MG glioma cells and immortalized astrocyte cells derived from an *Ink4a/Arf*-deficient mouse (hereafter, referred to as *Ink4a/Arf*$^{-/-}$ astrocytes) (Figure 2a). *Ink4a/Arf* is one of most frequently deleted tumor-suppressor genes in GBM. The expression levels of genes from the SHH (DVL1) and WNT ($\beta$-catenin, phosphorylated GSK3$\beta$, and cyclin D1) signaling pathways were not changed by KCTD2 depletion (Figure 2a). Previous studies by another group and by us showed that Cullin3 degrades cyclin E by polyubiquitination,[9,15] while in this study, KCTD2 depletion did not change cyclin E protein levels (Figure 2a). However, c-Myc, transcriptionally controlled by SHH and WNT signaling,[16,17] was increased by KCTD2 depletion (Figure 2a), indicating that KCTD2 regulates c-Myc protein levels independent of SHH and WNT signaling. To determine whether KCTD2 depletion changes c-Myc expression at a transcriptional level, we examined *c-Myc* mRNA levels using qRT-PCR. Our results showed no significant differences in *c-Myc* mRNA levels in KCTD2-depleted U87MG glioma cells and *Ink4a/Arf*$^{-/-}$ astrocytes (Figure 2b). We also examined whether Cullin3 had an effect on c-Myc protein levels. Cullin3 knockdown using a *Cullin3*-specific shRNA resulted in differences in c-Myc protein expression in both U87MG glioma cells and *Ink4a/Arf*$^{-/-}$ astrocytes (Figure 2c). Western blot analysis revealed that KCTD2 and c-Myc protein expression were inversely correlated in 7 out of 10 patients with GBM (Figure 2d). Thus, these results indicate that KCTD2 regulates c-Myc protein levels, but not mRNA levels.

To assess interactions between KCTD2 and c-Myc, Flag-tagged KCTD2 vectors and HA-tagged c-Myc vectors were transiently transfected in HEK 293 T cells. Western blot analysis showed that KCTD2 was detected in those proteins immunoprecipitated using an anti-HA antibody. Similarly, c-Myc was detected in those proteins immunoprecipitated using an anti-Flag antibody (Figure 3a). Next, we examined KCTD2-dependent c-Myc polyubiquitination. The results showed that c-Myc polyubiquitination was markedly increased either by KCTD2 overexpression or by treatment with lactacystin, a proteasome inhibitor, compared with that of c-Myc overexpression alone (Figure 3b). Furthermore, c-Myc polyubiquitination was further increased in the presence of both KCTD2 overexpression and lactacystin treatment (Figure 3b). We also examined the half-life of the c-Myc

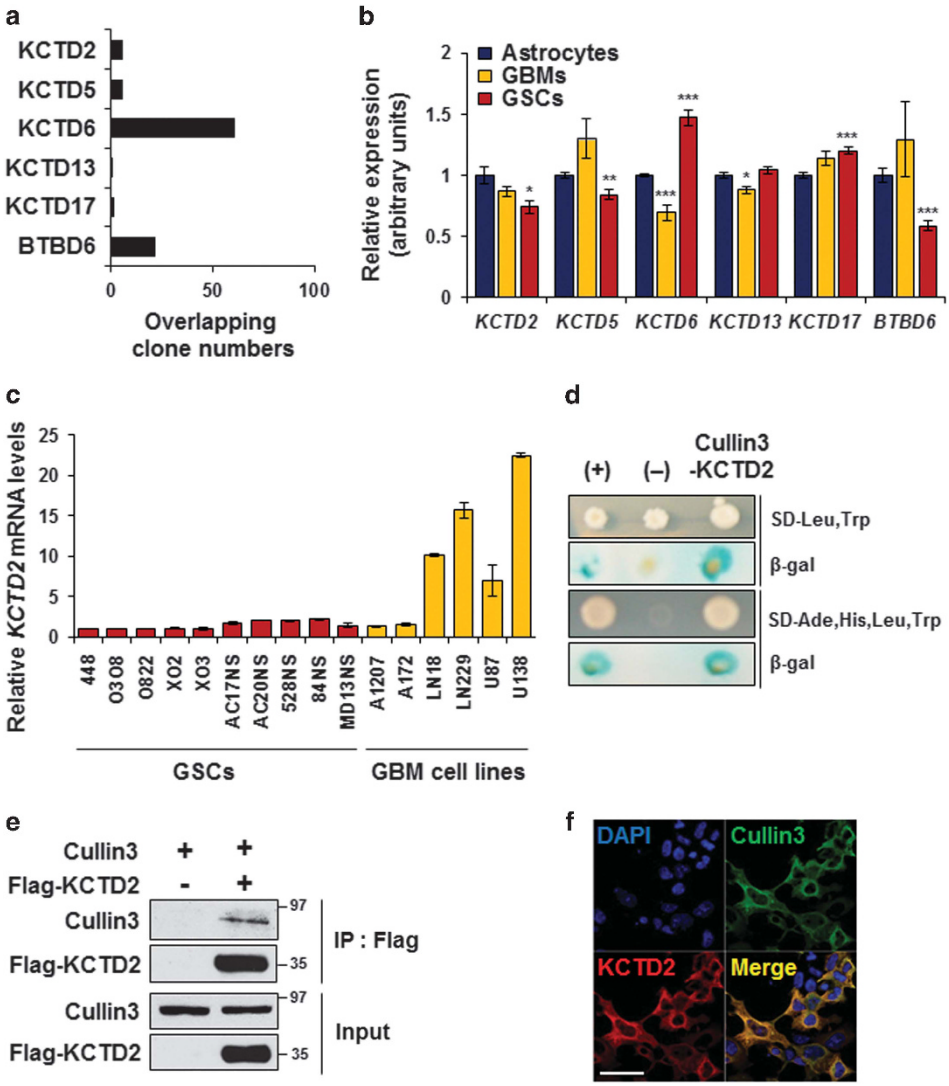


**Figure 1** Identification of KCTD2 as an adaptor of Cullin3 E3 ubiquitin ligase. (**a**) Overlapping clone numbers of Cullin3-binding proteins. Y2H screening was performed using Cullin3 as bait and a human fetal brain cDNA library. A total of 100 positive colonies were sequenced, of which sequence data of 98 samples were used, and 2 samples failed to sequence. (**b**) Relative mRNA expression levels of the *KCTD2, KCTD5, KCTD6, KCTD13, KCTD17, and BTBD6* genes were analyzed using transcriptome microarray data. Relative mRNA levels in astrocytes are set to 1. Normal astrocytes ($n=4$), GBMs ($n=5$), and GSCs ($n=7$). *$P<0.05$; **$P<0.01$; ***$P<0.001$. (**c**) Relative *KCTD2* mRNA levels in 10 GSCs and 6 GBM cell lines examined using qRT-PCR. (**d**) Interaction between KCTD2 and Cullin3 shown using a combination of selection medium and $\beta$-gal activity was verified using one-on-one Y2H analysis. Colony formation indicates effective plasmid transformation and positive $\beta$-gal staining represents an interaction. (+) indicates a positive control (pGBKT7-p53 and pGADT7-SV40), (–) indicates a negative control (pGBKT7, which contains only the DNA binding domain) , pGADT7 (which contains only the transactivation domain), and Cullin3-KCTD2 indicates pGBKT7-hCullin3 and pACT2-KCTD2. (**e**) Co-immunoprecipitation analysis was performed to determine an interaction between KCTD2 and Cullin3. pIRES-Cullin3 and pcDNA-Flag-KCTD2 plasmids were transfected in HEK 293 T cells. KCTD2 proteins were immunoprecipitated (IP) using an anti-Flag antibody followed by Cullin3 protein detection by western blot analysis using an anti-Cullin3 antibody. (**f**) Following transient transfection of pIRES-Cullin3 and pcDNA-Flag-KCTD2 plasmids in HEK 293 T cells, co-immunofluorescence analysis was performed to determine colocalization of KCTD2 (red) and Cullin3 (green). DAPI (blue) was used to stain nuclei. Scale bar represents 50 $\mu$m

protein in the presence or absence of KCTD2 overexpression using a cycloheximide chase assay and found that KCTD2 overexpression markedly reduced c-Myc protein half-life (Figure 3c). Collectively, these results show that KCTD2 interacts with the c-Myc protein and induces its degradation.

**KCTD2 depletion confers GSC properties to glioma cells by increasing c-Myc protein.** To determine whether the biologic effects of KCTD2 were dependent on c-Myc expression, we transfected a *c-Myc*-specific shRNA in KCTD2-depleted U87MG glioma cells and *Ink4a/Arf*$^{-/-}$ astrocytes (Figure 4a). We also established c-Myc-over-expressing cells as positive controls (Figure 4a). As decreased Cullin3 expression led to GSC self-renewal, we questioned whether KCTD2 was also involved in self-renewal and cancer stem cell marker expression. We first performed an *in vitro* limiting dilution assay to examine tumorsphere-forming ability, which is a surrogate marker for self-renewal of

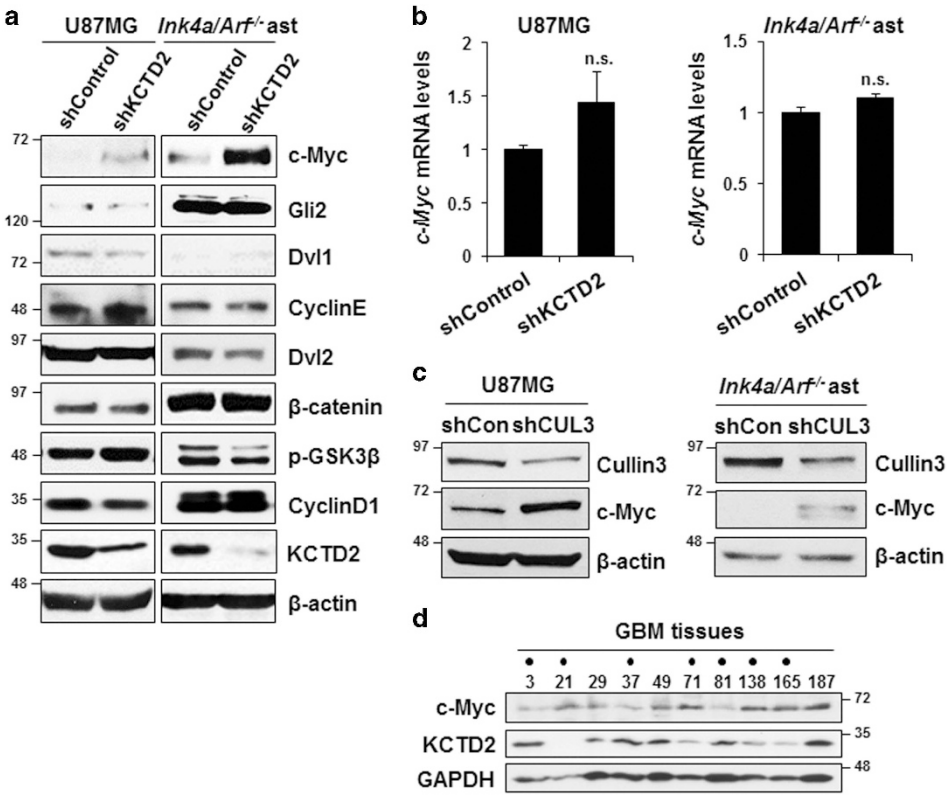


**Figure 2** KCTD2 depletion increases c-Myc protein levels but not c-Myc mRNA levels. (**a**) Expression of WNT and SHH signaling components and target genes in control (shControl) and KCTD2 knockdown (shKCTD2) in U87MG glioma cells and *Ink4a/Arf*$^{-/-}$ astrocytes were examined by western blot analysis. $\beta$-Actin was used as a loading control. (**b**) *c-Myc* mRNA levels in control (shControl) and KCTD2 knockdown (shKCTD2) in U87MG glioma cells and *Ink4a/Arf*$^{-/-}$ astrocytes were measured using qRT-PCR. NS indicates no significance. (**c**) Expression levels of c-Myc protein in control (shCon) and Cullin3 knockdown (shCul3) in U87MG glioma cells and *Ink4a/Arf*$^{-/-}$ astrocytes were examined by western blot analysis. $\beta$-Actin was used as a loading control. (**d**) Expression levels of KCTD2 and c-Myc proteins in protein extracts from GBM patient specimens were determined by western blot analysis. A closed dot (●) indicates GBM samples with a negative correlation between KCTD2 and c-Myc expression. Glyceraldehyde 3-phosphate dehydrogenase (GAPDH) was used as a loading control

cancer stem cells, in U87MG glioma cells and *Ink4a/Arf*$^{-/-}$ astrocytes. The results showed that KCTD2 depletion and c-Myc overexpression increased tumorsphere-forming ability in U87MG glioma cells and *Ink4a/Arf*$^{-/-}$ astrocytes (Figure 4b). The increased tumorsphere-forming ability in KCTD2-depleted cells was markedly attenuated by c-Myc knockdown (Figure 4b). These results indicate that KCTD2-mediated tumorsphere-forming ability was regulated by c-Myc protein. We also examined the expression of stem cell marker SOX2 (sex determining region Y-box2) and the glial marker GFAP (glial fibrillary acidic protein) in U87MG glioma cells and *Ink4a/Arf*$^{-/-}$ astrocytes. Fluorescence-activated cell sorting analysis showed that KCTD2 depletion or c-Myc overexpression increased SOX2 expression and decreased GFAP expression in both cell lines (Figure 4c). In addition, we found that these effects in KCTD2-depleted cells were restored by c-Myc knockdown (Figure 4c). Taken together, our results show that KCTD2 depletion regulates GSC features by increasing c-Myc protein.

To validate the effects of KCTD2 knockdown tumorigenesis *in vivo*, we performed intracranial injection of U87MG glioma cells in nude mice and found that KCTD2 knockdown or c-Myc overexpression significantly accelerated tumor growth compared with control cells (Figures 5a and b, upper left). We also found that increased tumor growth of KCTD2-depleted U87MG glioma cells was diminished by c-Myc knockdown (Figures 5a and b). In addition, immunohistochemical analysis showed that the number of cells expressing GFAP were markedly decreased, whereas the number of cells expressing Nestin and SOX2 was significantly increased in tumors from KCTD2-depleted or c-Myc-overexpressed U87MG glioma cells (Figures 5a and b). These changes in tumor growth and marker gene expression in KCTD2-depleted U87MG glioma cells were affected by c-Myc knockdown (Figures 5a and b). To summarize, our findings demonstrate that KCTD2 depletion promotes *in vivo* tumorigenesis through increases in the undifferentiated cell population by increasing c-Myc protein.

**KCTD2 depletion promotes glycolysis depending on c-Myc expression level.** c-Myc has an important role in aerobic glycolysis by activating glycolytic target genes, which is considered a crucial event for malignant transformation.[18,19] Therefore, we tested whether depletion of KCTD2 had an effect on glycolysis through c-Myc. We first measured glucose concentrations and lactate production in cell culture medium daily for 4 days. Glucose uptake was increased in KCTD2-depleted or c-Myc-overexpressed

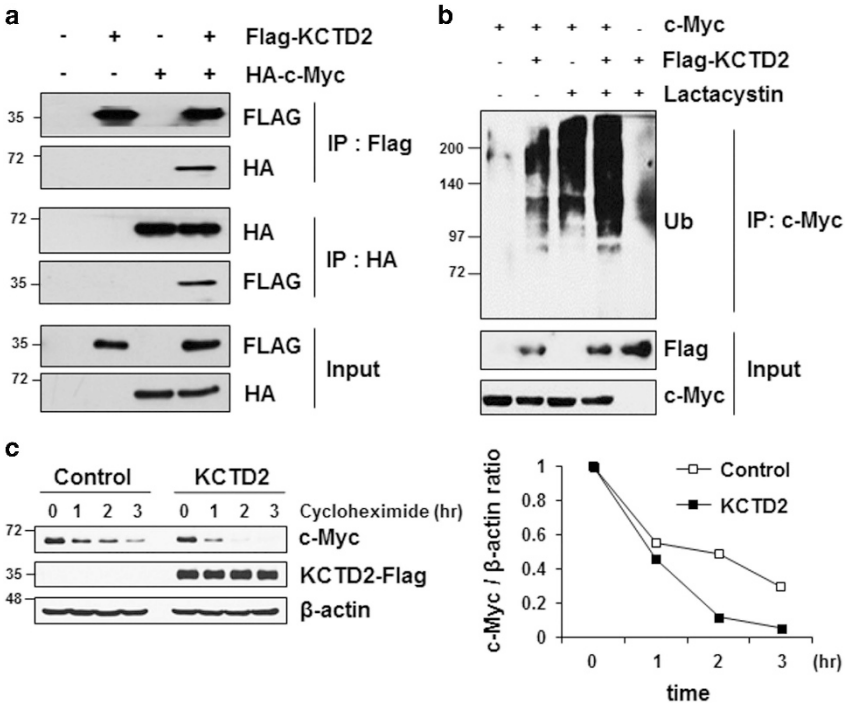


**Figure 3** KCTD2 interacts and degrades c-Myc protein. (**a**) pcDNA-HA-c-Myc and pcDNA-Flag-KCTD2 plasmids were transfected in HEK 293 T cells. Co-immunoprecipitation analysis was performed to examine interaction between KCTD2 and c-Myc. c-Myc protein was immunoprecipitated (IP) using an anti-HA antibody followed by KCTD2 detection by western blot analysis using an anti-Flag antibody. KCTD2 protein was immunoprecipitated using an anti-Flag antibody followed by c-Myc protein detection by western blot analysis using an anti-HA antibody. (**b**) Following plasmid transfection in HEK 293 T cells, polyubiquitination of c-Myc by KCTD2 was examined using western blot analysis. Cells were treated with DMSO or lactacystin (10 $\mu$M) for 6 h before protein extraction. (**c**) Reduction in c-Myc protein stability by ectopic KCTD2 expression in HEK 293 T cells was determined using a cycloheximide (CHX) chase assay. Quantitative values of the remaining c-Myc protein were measured using Image J software

U87MG glioma cells (Figure 6a). The increased glucose uptake found in KCTD2-depleted U87MG glioma cells was significantly reduced by c-Myc knockdown (Figure 6a). Similarly, lactate accumulation was markedly increased in KCTD2-depleted or c-Myc-overexpressed U87MG glioma cells (Figure 6b). The increased lactate accumulation found in KCTD2-depleted U87MG glioma cells was significantly decreased by c-Myc knockdown (Figure 6b). Furthermore, qRT-PCR analysis showed that KCTD2 depletion or c-Myc overexpression led to increased expression in genes involved in glucose uptake (glucose transporter 1; GLUT1) and glycolysis (ASC amino-acid transporter 2 (ASCT2), hexokinase 2 (HK2), enolase 1 (ENO1), lactate dehydrogenase A (LDHA), lactate dehydrogenase B (LDHB), phosphoinositide-dependent kinase 1 (PDK1), and monocarboxylate transporter 1 (MCT1)), all which are well-known target genes of c-Myc (Figure 6c). These changes in KCTD2-depleted cells were markedly restored by c-Myc knockdown (Figure 6c). Altogether, these results indicate that KCTD2 depletion activates aerobic glycolysis through changes in glycolytic metabolic gene expression by increasing c-Myc protein.

**KCTD2 and c-Myc gene signatures correlate with clinical outcomes of patients with malignant glioma.** To evaluate the clinical relevance of KCTD2 expression, we interrogated the Repository of Molecular Brain Neoplasia Data (REMBRANDT) data set.[20] *KCTD2* mRNA levels were decreased in astrocytoma, oligodendrocytoma, and GBM compared with non-tumors (Figure 7a). GBM was recently classified into four subtypes by gene expression profiles: neural, proneural, classical, and mesenchymal.[21] Among these subtypes, the proneural and neural subtypes are similar to a low-grade glioma, whereas the classical and mesenchymal subtypes are more similar to a higher grade glioma.[22] The classical and mesenchymal subtypes are known to be more aggressive than neural and proneural subtypes.[21] *KCTD2* mRNA was highly expressed in the neural subtype compared with the other subtypes, whereas its expression was lowest in the classical subtype (Figure 7b). To further delineate the significance of KCTD2-mediated regulation of c-Myc protein, we tested for correlations between *KCTD2* mRNA levels and c-Myc protein levels in patients with malignant glioma. As the REMBRANDT data set does not provide protein expression levels, c-Myc protein levels were substituted with a c-Myc gene signature (a combination of c-Myc's downstream target genes). *KCTD2* mRNA expression inversely correlated with the c-Myc gene signature but not with *c-Myc* mRNA levels (Figures 7c and d). There was no correlation between c-Myc mRNA levels and the c-Myc gene signature (Figure 7e). Among the Cullin3-binding adaptors identified using the Y2H assay (Figure 1a), only KCTD2 expression was negatively correlated with the c-Myc gene signature (data not shown). Furthermore, the c-Myc gene signature, not *c-Myc* mRNA levels, was strongly correlated with poor survival of patients with malignant glioma (Figures 7f and g). Patients with malignant glioma with

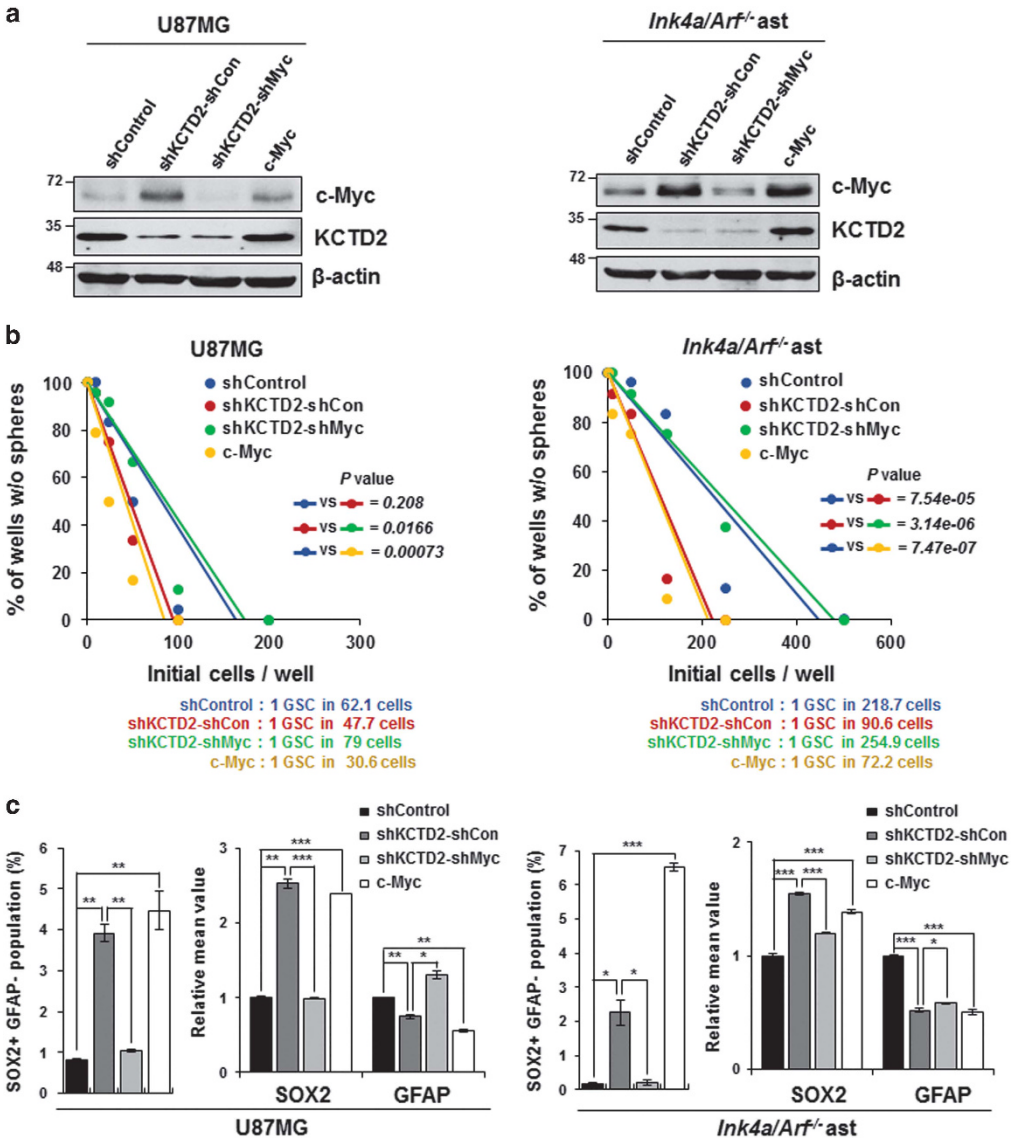


**Figure 4** KCTD2 depletion regulates GSC characteristics through increases in c-Myc protein. (**a**) Expression levels of KCTD2 and c-Myc in U87MG glioma cells and *Ink4a/Arf*$^{-/-}$astrocytes were examined using western blot analysis. $\beta$-Actin was used as a loading control. (**b**) Tumorsphere-forming abilities of U87MG glioma cells and *Ink4a/Arf*$^{-/-}$ astrocytes were determined using an *in vitro* limiting dilution assay. (**c**) Relative expression levels of the GSC marker SOX2 and the differentiated astrocyte marker GFAP in U87MG cells and *Ink4a/Arf*$^{-/-}$astrocytes as examined by FACS analysis. Evaluation of the cancer stem-like cells were assign using SOX2-FITC-positive and GFAP-PE-negative population. $^{*}P<0.05$; $^{**}P<0.01$; $^{***}P<0.001$

KCTD2-low/c-Myc gene signature-high showed worse survival than those with KCTD2-high/c-Myc signature-low (Figure 7h). Thus, our bioinformatics analysis showed that c-Myc protein expression and its transcriptional activity, rather than *c-Myc* mRNA levels, are significant indicators for survival prognosis of patients with malignant glioma. Taken together, the clinical significance of KCTD2 expression levels that are significantly lower in patients with aggressive glioma and are correlated with reduced survival may be attributed to increased c-Myc protein and transcriptional activity.

## Discussion

Recent studies have found a functional role of Cullin3 E3 ubiquitin ligase in different human malignancies. Genetic deregulation of the Cullin3 complex leads to activation of NF$\kappa$B signaling in patients with lung cancer,[23] and reduced Cullin3 expression was associated with human liver cancer progression.[24] The decreased Cullin3 by inhibitor of differentiation 1 induces stem cell properties in GBM by activating intracellular SHH and WNT through stabilization of GLI2 and DVL2, respectively.[9] Thus, Cullin3 is a key regulator of cancer progression. However, the underlying mechanisms and substrate recognition specificity of Cullin3 are not fully understood. Therefore, in this study, we carried out Y2H screening to identify Cullin3-interacting BTB domain proteins.

Among the binding partners with Cullin3 in Figure 1a, it has been found that KCTD6, KCTD13, and BTB domain-containing 6 (BTBD6) are well-characterized adaptors for the Cullin3 complex. For example, KCTD6–Cullin3 complex

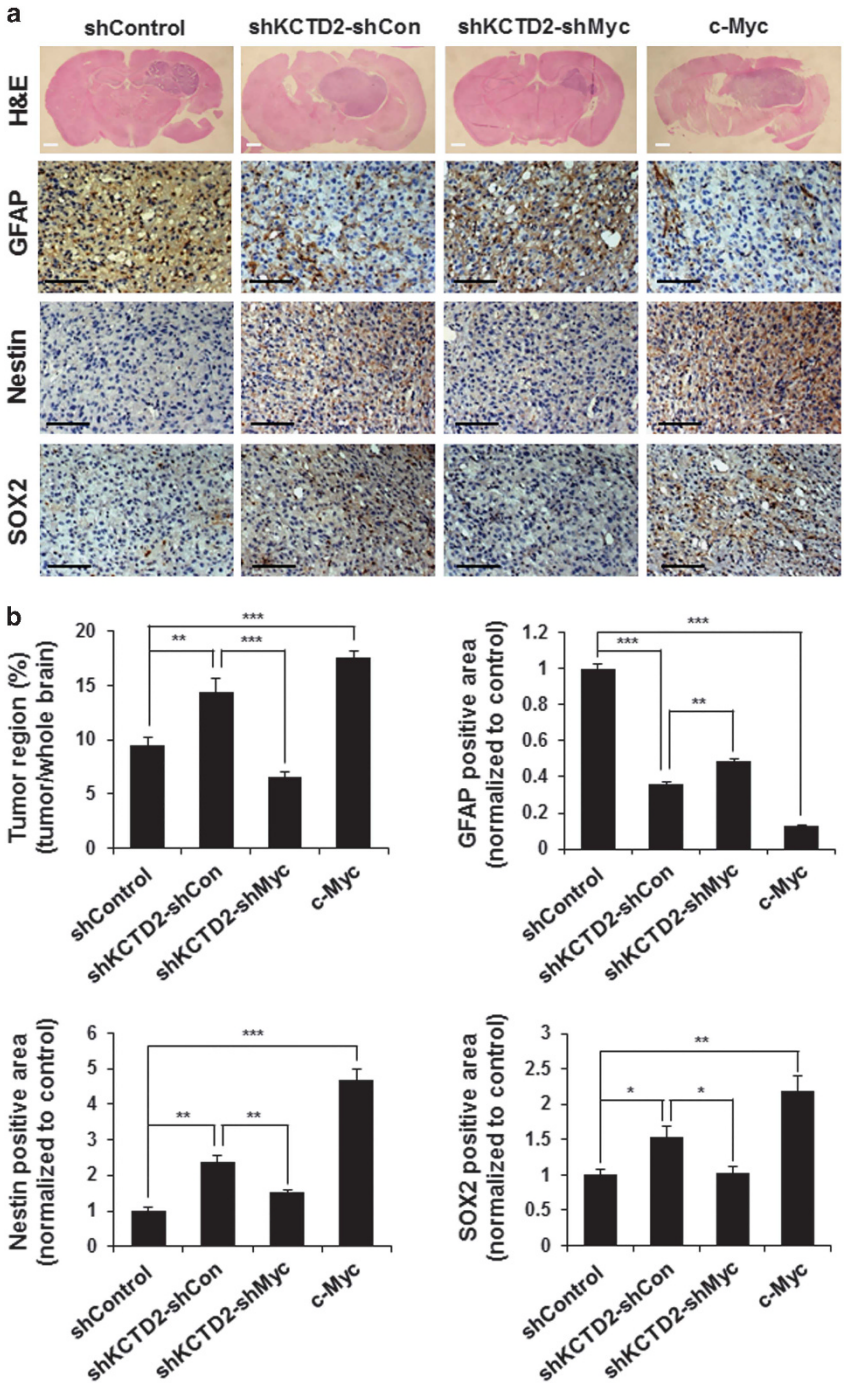


**Figure 5** KCTD2 depletion stimulates tumor growth as shown by an increase of the undifferentiated glioma cell population *in vivo*. (**a**) Representative H&E staining and immunohistochemistry data were obtained from mouse intracranial xenografts of the respective cells. Immunohistochemistry analysis showed expression of the differentiated astrocyte marker (GFAP) and the stem cell markers (Nestin and SOX2). White scale bar represents 500 $\mu$m and black scale bar represents 100 $\mu$m. (**b**) Quantitative data for tumor region (upper left) and positively stained areas of GFAP (upper right), Nestin (lower left), and SOX2 (lower right) were obtained from results shown in panel **a**. $^{*}P<0.05$; $^{**}P<0.01$; $^{***}P<0.001$

promoted the degradation of small ankyrin-1 in the cardiomyocytes as well as HDAC1 protein in the pediatric malignant primary brain tumor.[25,26] Moreover, KCTD13 and BTBD6 downregulated the protein stability of RhoA and Plzf via the interaction with Cullin3, respectively.[27,28] In contrast, we found no evidence that Cullin3 interacts with KCTD2 protein as a BTB domain adaptor.

According to expression pattern of KCTD2 that is low in GSCs compared with glioma cells, we depleted KCTD2 expression in glioma cells and immortalized astrocyte, and

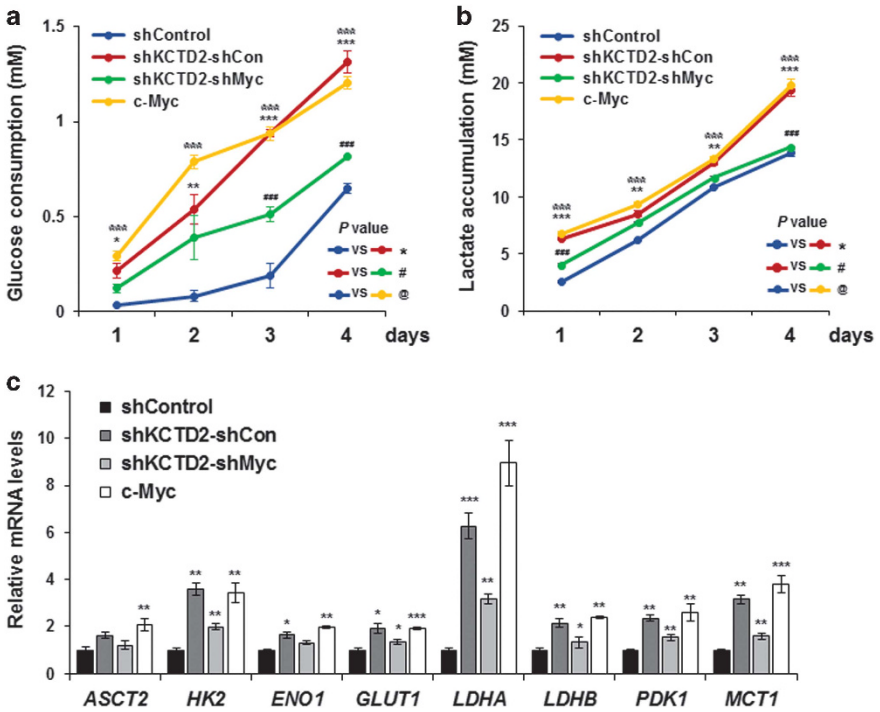


**Figure 6** KCTD2 depletion induces aerobic glycolysis through c-Myc regulation. (**a**) Glucose levels in cells were determined using a GO assay kit at the indicated times. Glucose consumption was determined as the difference in glucose concentration in the culture medium compared with control. *, $^{@}$, and $^{\#}P<0.05$; **, $^{@@}$, and $^{\#\#}P<0.01$; ***, $^{@@@}$, and $^{\#\#\#}P<0.001$. (**b**) Lactate concentration in culture medium of the indicated U87MG glioma cells was measured at the indicated time using an L-lactate assay kit. *, $^{@}$, and $^{\#}P<0.05$; **, $^{@@}$, and $^{\#\#}P<0.01$; ***, $^{@@@}$, and $^{\#\#\#}P<0.001$. (**c**) The mRNA levels of glycolysis-related genes, *ASCT2*, *HK2*, *ENO1*, *GLUT1*, *PDK1*, *LDHA*, and *MCT1*, in the indicated U87MG glioma cells were measured using qRT-PCR. $^{*}P<0.05$; $^{**}P<0.01$; $^{***}P<0.001$

found that a loss of KCTD2 induces c-Myc stability and tumor growth. Thus, it is likely that KCTD2 depletion-dependent tumorigenesis is primarily attributed to c-Myc because c-Myc knockdown in KCTD2-depleted cells completely reverses the tumorigenic effect of KCTD2.

c-Myc is highly expressed in embryonic stem cells and can generate induced pluripotent stem cells.[29] A recent study found that c-Myc is required for diverse features of GSCs.[12] c-Myc is dysregulated by c-Myc gene amplification in malignant gliomas and its c-Myc nuclear expression levels are associated with increased tumor aggressiveness.[30] Similarly, our bioinformatics analysis using the REMBRANDT data set revealed that c-Myc transcription activity, as determined by the c-Myc gene signature, but not c-Myc mRNA levels, is correlated with worse survival of patients with malignant gliomas. These results suggest that regulation of c-Myc protein levels rather than its mRNA levels is more critical for its function in malignant glioma pathogenesis. Therefore, increased c-Myc protein stability by decreased KCTD2 is a critical mechanism to regulate its transcriptional activity and effects on aerobic glycolysis, self-renewal, and tumor growth.

Several studies have demonstrated that c-Myc protein stability is regulated by phosphorylation. The RAF–MEK–ERK pathway stabilizes the c-Myc protein by phosphorylation at serine 62, whereas protein phosphatase 2 promotes ubiquitination-mediated degradation of c-Myc by dephosphorylation at serine 62.[31] A recent study demonstrated that FBW7 ubiquitin ligase has an important role in tumor suppression. One of the molecular mechanisms underlying the tumor suppression function of FBW7 ligase is degradation of c-Myc protein. FBW7 ligase regulates c-Myc protein degradation by recognizing phosphorylation of c-Myc at threonine 58. However, mutation of c-Myc at threonine 58 was frequently detected in several cancers.[31] Although cancers containing this mutation are not affected by this c-Myc inactivation mechanism, which results in the accumulation of c-Myc protein and accelerated tumor progression. c-Myc protein is also increased in several tumors that have mutations in FBW7.[32] Therefore, understanding other mechanisms governing c-Myc inactivation is essential to establishing a therapeutic modality targeting c-Myc in various human malignancies. In the present report, we showed that the BTB domain-containing KCTD2 adaptor interacts with Cullin3 ubiquitin ligase and the c-Myc protein, and induces c-Myc protein degradation. KCTD2 expression is lower in GSCs compared with glioma cells, and depletion of KCTD2 leads to tumorigenic properties by increasing c-Myc protein. Therefore, the molecular mechanism governing c-Myc activity by the Cullin3–KCTD2 complex is important for c-Myc stability in malignant gliomas, and may provide an alternative strategy for targeting the c-Myc protein (Figure 7i).

## Materials and Methods

**Y2H library screening.** Y2H screening was performed as described previously.[33] Briefly, the bait vector pGBKT7-Cullin3 was transformed in yeast

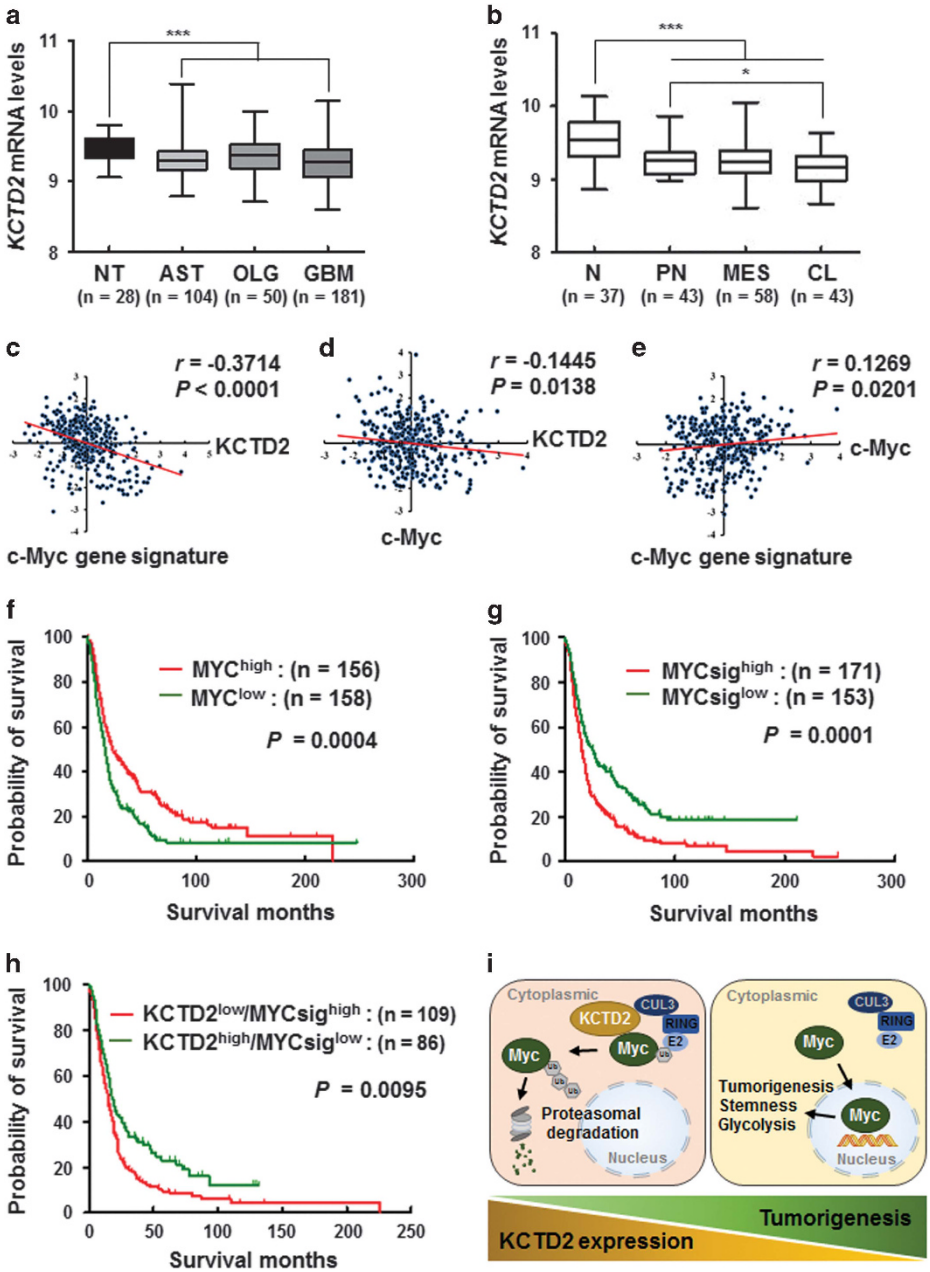


**Figure 7** KCTD2 and c-Myc gene signature correlates with clinical outcomes of patients with malignant glioma. (**a**) Relative *KCTD2* mRNA levels in non-tumor (NT), astrocytoma (AST), oligodendrocytoma (OLG), and GBM were obtained from the REMBRANDT data set. ***$P<0.001$. (**b**) Relative *KCTD2* mRNA levels in four different GBM subtypes were analyzed using the REMBRANDT data set. Neural (N), Proneural (PN), Mesenchymal (MES), and Classical (CL). *$P<0.05$; ***$P<0.001$. (**c**) Correlation of *KCTD2* mRNA levels *versus* c-Myc gene signature, (**d**) *KCTD2* mRNA levels *versus* *c-Myc* mRNA levels, and (**e**) *c-Myc* mRNA levels *versus* c-Myc gene signature, were analyzed using the REMBRANDT data set. (**f–h**) Kaplan–Meier survival data of patients with malignant glioma were obtained from the REMBRANDT data set. Kaplan–Meier survival analysis was performed between patient groups based on: (**f**) *c-Myc* mRNA-high *versus* *c-Myc* mRNA-low, (**g**) *c-Myc* gene signature-high *versus* c-Myc gene signature-low, and (**h**) *KCTD2* mRNA-low/c-Myc gene signature-high *versus* *KCTD2* mRNA-high/c-Myc gene signature-low. (**i**) A schematic diagram showing c-Myc ubiquitination by Cullin3-KCTD2 complex in malignant gliomas

strain *Saccaromyes cerevisiae AH109* using the LiAc/polyethylene glycol method and then used to screen a pretransformed MATCHMAKER human fetal brain library (Clontech, Palo Alto, CA, USA), cloned in pACT2, by mating with the yeast strain Y187.

**REMBRANDT data analysis.** The REMBRANDT data set was used to identify correlations between clinical characteristics, gene expression, and survival of KCTD2 and c-Myc in glioma specimens. First, clinical 'information-lacking tumor samples' ($n=199$, including unknown, mixed, survival information-lacked) were excluded from the REMBRANDT data set ($n=534$), with the remaining samples named 'tumor type-recorded glioma'. Second, tumor samples that did not have tumor grade information ($n=21$) were excluded from the tumor type-recorded glioma set ($n=335$), and were named 'second group'. Patient samples in the second group ($n=314$) were used to analyze KCTD2 gene expression in

non-tumor, astrocytoma, oligodendroglioma, and GBM, as well as in four GBM subtypes (neural, proneural, mesenchymal, and classical). The c-Myc gene signature group was collected from HALLMARK_MYC_TARGETS_V1 in MSigDB of the GSEA website (http://software.broadinstitute.org/gsea/index.jsp). Patient groups were divided according to being above or below the mean c-Myc, c-Myc gene signature, and KCTD2 expression levels for survival analysis.

**Cell lines and culture conditions.** Human glioma cell line U87MG was purchased from the American Type Culture Collection (ATCC, Manassas, VA, USA). U87MG glioma cells and *Ink4a/Arf*$^{-/-}$ astrocytes were cultured in Dulbecco's modified Eagle's medium (DMEM) with high glucose (4500 mg/l) supplemented with 10% fetal bovine serum (Serana, Bunbury, Australia), 1% penicillin/streptomycin (Thermo Scientific, Rockford, IL, USA), and 2 mM L-glutamine (Thermo Scientific). For *in vitro* limiting dilution assay, U87MG glioma cells and *Ink4a/Arf*$^{-/-}$ astrocytes were cultured in DMEM/F12 supplemented with B27 (Invitrogen, Carlsbad, CA, USA), EGF (20 ng/ml; R&D Systems, Minneapolis, MN, USA), and bFGF (20 ng/ml; R&D Systems).

**Plasmid transfection, shRNA construction, and gene transduction.** Cells were directly transfected with pIRES-Cullin3, pcDNA3.1-Flag-KCTD2, and pcDNA3-HA-c-Myc expression vectors using a Neon microporation kit (Invitrogen). shCullin3 (5′-AAGTTGTACGGTATGGGT-3′), shKCTD2 (5′-TCA TAGAGCCGAGCGAAAT-3′), and shMyc (5′-CAGTTGAAACACAAACTTGAA-3′) were cloned into the pSuperRetro-puro and pSuperRetro-GFP-neo vectors according to the manufacturer's instructions (Oligoengine, Seattle, WA, USA) and directly transfected into glioma cells using a Neon microporation kit (Invitrogen).

**Quantitative real-time PCR.** One microgram of DNase I-treated RNA was reverse-transcribed into cDNA using a RevertAid first-strand cDNA synthesis kit (Fermentas, Glen Burnie, MD, USA) according to the manufacturer's instructions. qRT-PCR analysis was performed using an iCycler IQ Real-Time PCR Detection System (Bio-Rad, Hercules, CA, USA) using an IQ Supermix with SYBR-Green (Takara, Tokyo, Japan).

**Co-immunoprecipitation and western blot analyses.** For co-immunoprecipitation assay, HEK 293 T cells were co-transfected with the previously described constructs, protein was extracted using NP-40 lysis buffer (50 mM Tris-HCl (pH 7.4), 150 mM NaCl, 1% NP40, 1 mM EDTA, and protease inhibitor (Roche Diagnostics, Mannheim, Germany)). Co-immunoprecipitation was performed using the anti-Flag M2 antibody (Sigma-Aldrich, St. Louis, MO, USA) and the anti-HA antibody (Covance, Berkeley, CA, USA). For the ubiquitination assays, cells were treated with lactacystin (5 $\mu$M; Sigma-Aldrich) for 6 h before collection.

Whole-cell extracts were prepared using RIPA lysis buffer (50 mM Tris-HCl (pH 7.4), 150 mM NaCl, 1% NP-40, and 0.1% sodium dodecyl sulfate (SDS)) containing 1 mM $\beta$-glycerophosphate, 2.5 mM sodium pyrophosphate, 1 mM NaF, 1 mM $Na_3VO_4$, and protease inhibitor (Roche Diagnostics). Proteins were quantified using the Bradford assay reagent (Bio-Rad) according to the manufacturer's instructions. Proteins (30–100 $\mu$g) were separated by 10% SDS-polyacrylamide gel electrophoresis and transferred to polyvinylidene fluoride membranes (Pall, New York, NY, USA). Membranes were blocked using 5% non-fat milk and incubated with primary antibodies. Membranes were then incubated with horseradish peroxidase-conjugated secondary antibodies and visualized using the SuperSignal West Pico Chemiluminescent Substrate (Elpis Biotech, Daejeon, Korea).

**Cycloheximide chase assay.** HEK 293 T cells were transfected with Flag-tagged KCTD2. At 48 h post- transfection, 50 $\mu$g/ml cycloheximide was added to the medium, and cells were harvested at the indicated time points. Quantitative c-Myc expression relative to $\beta$-actin levels was analyzed using Image J (Version 1.45 (NIH, Bethesda, MD, USA)).

**Glucose consumption and lactate production.** Cells were seeded in culture dishes, and culture medium was collected for measurement of glucose and lactate concentrations at indicated days. Glucose levels were determined using a Glucose (GO) assay kit (Sigma-Aldrich). Glucose consumption was determined as the difference in glucose concentration compared with control. Lactate levels were measured using the L-lactate assay kit (Eton-Bioscience, San Diego, CA, USA).

**Immunofluorescence and immunohistochemistry assays.** HEK 293 T cells were transfected with Cullin3 and KCTD2 expression plasmids and subsequently fixed using 4% paraformaldehyde. Fixed cells were incubated with primary antibodies for 12 h at 4 °C. Nuclei were stained using 4′,6-diamidino-2-phenylindole (DAPI, 1 $\mu$g/ml) for 5 min. Fluorescence images were obtained using a confocal laser scanning LSM 5 Pascal microscope (Carl Zeiss, Jena, Germany). Mouse brain tissues embedded in paraffin were sliced into 5 $\mu$m thick sections. Immunohistochemistry staining of tumor sections was done using the Vectastain ABC Kit (Vector Laboratories, Burlingame, CA, USA). Sections were examined using optical and confocal microscopy (Carl Zeiss). Information on the antibodies used for immunofluorescence and immunohistochemistry are available upon request. Regions of immunoperoxidase-stained cells in brain tissue were quantitatively measured using Metamorph threshold analysis (Version 7.1.0.0, Molecular Devices Inc., Sunnyvale, CA, USA).

**FACS analysis.** Cells were dissociated into single cells using Trypsin-EDTA (Sigma-Aldrich), washed, and suspended in phosphate-buffered saline (PBS). Cells were fixed using 4% paraformaldehyde and subsequently permeabilized using 0.1% BSA, 1% serum, and 1% Triton. For analysis of target protein expression, cells were stained with the respective primary antibody such as anti-Nestin (Sigma-Aldrich), anti-SOX2 (R&D Systems), anti-CD133 (Miltenyi Biotec, Bergisch Gladbach, Germany), and anti-GFAP (MP Biomedicals, Santa Ana, CA, USA), followed by incubation with a biotin-conjugated secondary antibody and PE-conjugated avidin (BD Pharmingen, San Diego, CA, USA). Fluorescence intensities were measured using FACS Verse (BD Pharmingen, San Jose, CA, USA).

***In vitro* limiting dilution sphere formation assay.** For the *in vitro* limiting dilution assay, a decreasing number of cells (500, 250, 100, 50, and 10) were manually seeded per well in 96-well plates containing DMEM/F12 with B27, EGF, and bFGF ($n=18$). Neurospheres larger than 10 $\mu$m in diameter were counted by light microscopy after 14 days. Stem cell frequency was calculated using ELDA software available at http:bioinf.wehi.edu.au/software/elda.[34]

**Intracranial injection assay.** U87MG glioma cells were harvested by trypsinization, washed with PBS, and cell viability was determined by Trypan blue exclusion. Single-cell suspensions with $>90\%$ viability were used for *in vivo* studies. Cells ($5\times10^4$ in 3 $\mu$l of PBS) were stereotactically injected into the left striatum of 6-week-old BALB/c nu/nu mice (coordinates relative to the bregma: anterior–posterior +2 mm, medial–lateral +2 mm, and dorsal–ventral −3 mm). Mice whose body weight had decreased by $>25\%$ were considered to have an intracranial tumor. Mice harboring tumors were perfused with PBS and 4% paraformaldehyde. Intracranial tumor tissues were embedded in paraffin, sectioned (4 $\mu$m thickness) and stained with hematoxylin and eosin (H&E) at histologically similar positions. Intracranial tumor size was measured using MetaMorph software. The total brain area was divided by H&E-stained tumor regions. All animal experiments were approved by the animal care committee of Korea University (Seoul, Republic of Korea), and were performed in accordance with government and institutional guidelines and regulations.

**Statistical analysis.** Data were analyzed using a two-tailed Student's *t*-test. *P* values $<0.05$ (indicated by $^{*,\ \#,\ @}$), $<0.01$ (indicated by $^{**,\ \#\#,\ @@}$) and $<0.001$ (indicated by $^{***,\ \#\#\#,\ @@@}$) were considered statistically significant. Data were presented as the mean $\pm$ S.D.

## Conflict of Interest

The authors declare no conflict of interest.

**Acknowledgements**. We thank all members of Cell Growth Regulation Lab for their helpful discussions and technical assistances. This work was supported by grants from the National Research Foundation (NRF) funded by the Ministry of Science, ICT and Future Planning (2011-0017544, 2015R1A5A1009024 and 2016R1D1A1B03931941), from Next-Generation Biogreen21 Program (PJ01107701), from the General Program of the National Natural Science Foundation of China (no. 81572891), and from Korea University.

1. Hershko A, Ciechanover A. The ubiquitin system. *Annu Rev Biochem* 1998; **67**: 425–479.
2. Sarikas A, Hartmann T, Pan ZQ. The cullin protein family. *Genome Biol* 2011; **12**: 220.
3. Genschik P, Sumara I, Lechner E. The emerging family of CULLIN3-RING ubiquitin ligases (CRL3s): cellular functions and disease implications. *EMBO J* 2013; **32**: 2307–2320.

4. Furukawa M, He YJ, Borchers C, Xiong Y. Targeting of protein ubiquitination by BTB-Cullin 3-Roc1 ubiquitin ligases. *Nat Cell Biol* 2003; **5**: 1001–1007.
5. Smaldone G, Pirone L, Balasco N, Di Gaetano S, Pedone EM, Vitagliano L. Cullin 3 recognition is not a universal property among KCTD proteins. *PLoS One* 2015; **10**: e0126808.
6. Wen PY, Kesari S. Malignant gliomas in adults. *N Engl J Med* 2008; **359**: 492–507.
7. Vescovi AL, Galli R, Reynolds BA. Brain tumor stem cells. *Nat Rev Cancer* 2006; **6**: 425–436.
8. Stopschinski BE, Beier CP, Beier D. Glioblastoma cancer stem cells – from concept to clinical application. *Cancer Lett* 2013; **338**: 32–40.
9. Jin X, Jeon HM, Jin X, Kim EJ, Yin J, Jeon HY *et al.* ID1-Cullin3 axis regulates intracellular SHH and WNT signaling in glioblastoma stem cells. *Cell Rep* 2016; **16**: 1629–1641.
10. Eilers M, Eisenman RN. Myc's broad reach. *Genes Dev* 2008; **22**: 2755–2766.
11. Nesbit CE, Tersak JM, Prochownik EV. MYC oncogenes and human neoplastic disease. *Oncogene* 1999; **18**: 3004–3016.
12. Wang J, Wang H, Li Z, Wu Q, Lathia JD, McLendon RE *et al.* c-Myc is required for maintenance of glioma cancer stem cells. *PLoS One* 2008; **3**: e3769.
13. Mao P, Joshi K, Li J, Kim SH, Li P, Santana-Santos L *et al.* Mesenchymal glioma stem cells are maintained by activated glycolytic metabolism involving aldehyde dehydrogenase 1A3. *Proc Natl Acad Sci USA* 2013; **110**: 8644–8649.
14. Bennett EJ, Rush J, Gygi SP, Harper JW. Dynamics of cullin-RING ubiquitin ligase network revealed by systematic quantitative proteomics. *Cell* 2010; **143**: 951–965.
15. Singer JD, Gurian-West M, Clurman B, Roberts JM. Cullin-3 targets cyclin E for ubiquitination and controls S phase in mammalian cells. *Genes Dev* 1999; **13**: 2375–2387.
16. He TC, Sparks AB, Rago C, Hermeking H, Zawel L, da Costa LT *et al.* Identification of c-Myc as a target of the APC pathway. *Science* 1998; **281**: 1509–1512.
17. Karhadkar SS, Bova GS, Abdallah N, Dhara S, Gardner D, Maitra A *et al.* Hedgehog signaling in prostate regeneration, neoplasia and metastasis. *Nature* 2004; **431**: 707–712.
18. Dang CV, Le A, Gao P. MYC-induced cancer cell energy metabolism and therapeutic opportunities. *Clin Cancer Res* 2009; **15**: 6479–6483.
19. Vander Heiden MG, Cantley LC, Thompson CB. Understanding the Warburg effect: the metabolic requirements of cell proliferation. *Science* 2009; **324**: 1029–1033.
20. Madhavan S, Zenklusen JC, Kotliarov Y, Sahni H, Fine HA, Buetow K. Rembrandt: helping personalized medicine become a reality through integrative translational research. *Mol Cancer Res* 2009; **7**: 157–167.
21. Verhaak RG, Hoadley KA, Purdom E, Wang V, Qi Y, Wilkerson MD *et al.* Integrated genomic analysis identifies clinically relevant subtypes of glioblastoma characterized by abnormalities in PDGFRA, IDH1, EGFR, and NF1. *Cancer Cell* 2010; **17**: 98–110.
22. Guan X, Vengoechea J, Zheng S, Sloan AE, Chen Y, Brat DJ *et al.* Molecular subtypes of glioblastoma are relevant to lower grade glioma. *PLoS One* 2014; **9**: e91216.
23. Thu KL, Pikor LA, Chari R, Wilson IM, Macaulay CE, English JC *et al.* Genetic disruption of KEAP1/Cul3 E3 ubiquitin ligase complex components is a key mechanism of NF-kappaB pathway activation in lung cancer. *J Thorac Oncol* 2011; **6**: 1521–1529.
24. Kossatz U, Breuhahn K, Wolf B, Hardtke-Wolenski M, Wilkens L, Steinemann D *et al.* The cyclin E regulator cullin 3 prevents mouse hepatic progenitor cells from becoming tumor-initiating cells. *J Clin Invest* 2010; **120**: 3820–3833.
25. Lange S, Perera S, Teh P, Chen J. Obscurin and KCTD6 regulate cullin-dependent small ankyrin-1 (sAnk1.5) protein turnover. *Mol Biol Cell* 2012; **23**: 2490–2504.
26. De Smaele E, Di Marcotullio L, Moretti M, Pelloni M, Occhione MA, Infante P *et al.* Identification and characterization of KCASH2 and KCASH3, 2 novel Cullin3 adaptors suppressing histone deacetylase and Hedgehog activity in medulloblastoma. *Neoplasia* 2011; **13**: 374–3850.
27. Chen Y, Yang Z, Meng M, Zhao Y, Dong N, Yan H *et al.* Cullin mediates degradation of RhoA through evolutionarily conserved BTB adaptors to control actin cytoskeleton structure and cell movement. *Mol Cell* 2009; **35**: 841–855.
28. Sobieszczuk DF, Poliakov A, Xu Q, Wilkinson DG. A feedback loop mediated by degradation of an inhibitor is required to initiate neuronal differentiation. *Genes Dev* 2010; **24**: 206–218.
29. Araki R, Hoki Y, Uda M, Nakamura M, Jincho Y, Tamura C *et al.* Crucial role of c-Myc in the generation of induced pluripotent stem cells. *Stem Cells* 2011; **29**: 1362–1370.
30. Faria MH, Khayat AS, Burbano RR, Rabenhorst SH. c -MYC amplification and expression in astrocytic tumors. *Acta Neuropathol* 2008; **116**: 87–95.
31. Yeh E, Cunningham M, Arnold H, Chasse D, Monteith T, Ivaldi G *et al.* A signaling pathway controlling c-Myc degradation that impacts oncogenic transformation of human cells. *Nat Cell Biol* 2004; **6**: 308–318.
32. Welcker M, Clurman BE. FBW7 ubiquitin ligase: a tumour suppressor at the crossroads of cell division, growth and differentiation. *Nat Rev Cancer* 2008; **8**: 83–93.
33. Kim SH, Park J, Choi MC, Kim HP, Park JH, Jung Y *et al.* Zinc-fingers and homeoboxes 1 (ZHX1) binds DNA methyltransferase (DNMT) 3B to enhance DNMT3B-mediated transcriptional repression. *Biochem Biophys Res Commun* 2007; **2**: 318–323.
34. Kim SH, Kim EJ, Hitomi M, Oh SY, Jin X, Jeon HM *et al.* The LIM-only transcription factor LMO2 determines tumorigenic and angiogenic traits in glioma stem cells. *Cell death Differ* 2015; **22**: 1517–1525.